

Activation energies of the amorphous-crystalline transformation in the $\text{Fe}_{40}\text{Ni}_{40}\text{P}_{14}\text{B}_6$ metallic alloy

M. A. ZAKI EWISS, S. SALEH

Physics Department, Faculty of Applied Science, Orman University of Cairo, Gameet et Kahira Street, Giza, Egypt

The amorphous – crystalline phase change of the metallic glass $\text{Fe}_{40}\text{Ni}_{40}\text{P}_{14}\text{B}_6$ has been studied by examining the change in the electric resistivity, using isochronal and isothermal heating. The isochronal measurements indicate that the crystallization occurs in two stages. One stage appears as a change with pre-annealing in the height of the resistivity–temperature curve at 600 K. This stage characterizes an induction period for recrystallization activated by $(1.46 + 0.03)$ eV. The other stage, occurring at temperature above 600 K and manifesting itself as a remarkable drop in the resistivity indicates the onset of crystallization. From the isothermal studies of this stage, the energy activating the crystallization is found to be $(3.58 + 0.03)$ eV. The minimum energy activating the vacancy formation in the crystallized matrix has been calculated to be $(1.96 + 0.03)$ eV. These results are compared with the corresponding data obtained for the amorphous and crystalline metallic glasses $\text{Fe}_{40}\text{Ni}_{40}\text{B}_{20}$ and $\text{Fe}_{32}\text{Ni}_{36}\text{Cr}_{14}\text{P}_{12}\text{B}_6$.

1. Introduction

The ferromagnetic materials $\text{Fe}_{40}\text{Ni}_{40}\text{B}_{20}$, $\text{Fe}_{40}\text{Ni}_{40}\text{P}_{14}\text{B}_6$ and $\text{Fe}_{32}\text{Ni}_{36}\text{Cr}_{14}\text{P}_{12}\text{B}_6$ are important for many industrial applications, because of their hardness, creep and high resistance. These materials are obtained by rapid quenching. Therefore, they are structurally unstable in the “as-quenched” state. Consequently, their physical properties are significantly changed by annealing treatment even before crystallization.

Nowadays, extensive experimental and theoretical studies of the structural changes responsible for these effects have been accumulated in literature ([1–5] and the references therein), aiming not only to obtain desirable physical properties but also to control the long-term stability of the amorphous alloys as engineering materials.

In a previous report [6], an explanation of the anomalous features occurring during the amorphous–crystalline transition of the $\text{Fe}_{40}\text{Ni}_{40}\text{B}_{20}$ and $\text{Fe}_{32}\text{Ni}_{36}\text{Cr}_{14}\text{P}_{12}\text{B}_6$ amorphous alloys have been discussed. As far as we know, information on the $\text{Fe}_{40}\text{Ni}_{40}\text{P}_{14}\text{B}_6$ glassy metallic alloy is lacking in the literature. For this reason, this work was carried out to study the amorphous–crystalline phase change of the metallic glass $\text{Fe}_{40}\text{Ni}_{40}\text{P}_{14}\text{B}_6$, using resistivity changes as the tool of the study.

2. Experimental procedure

The material used was prepared and supplied in the form of flexible ribbons of an average thickness 0.2 mm and width 1.5 mm. Test samples each of length

20 mm, were cut from the same ribbon. The electrical resistivity measurements were carried out using the conventional four-probe apparatus. The current probes connected with constant current source and the voltage drop were measured using a conventional potentiometer.

3. Results and discussion

In a previous work [6], it was shown that the electrical resistivity changes with temperature in two different regions, corresponding to the induction stage prior to crystallization and the crystallization stage including the vacancy formation in the crystallized matrix. In order to determine the activation energies characterizing these matrices, three samples of the amorphous alloy under study were used for each stage and were treated by annealing as detailed below.

3.1. The induction stage prior to crystallization

To determine the energy activating the induction stage before crystallization of the $\text{Fe}_{40}\text{Ni}_{40}\text{P}_{14}\text{B}_6$ amorphous alloy, the three samples (as-received) were isochronally annealed for 10 min at each temperature of 590, 600 and 610 K. In every case, the electrical resistivity (ρ) was measured as a function of temperature. The results for the isochronal annealing at the above-mentioned temperatures are shown in Fig. 1. It is worth noting that a remarkable decrease in the peak height of the resistivity was observed on increasing the annealing temperature. Previously [6], it was mentioned that the decrease in resistivity could be taken to

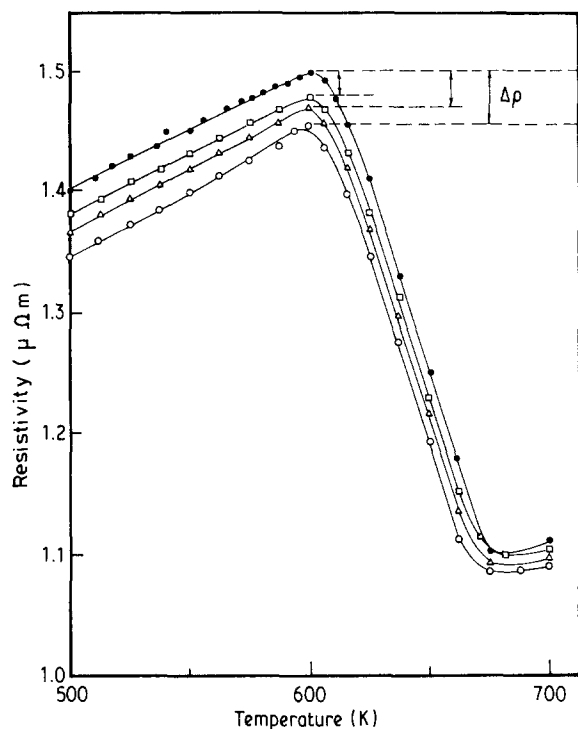


Figure 1 Effect of pre-annealing at temperature below the crystallization temperature on the change of the electrical resistivity with temperature through the induction stage of the amorphous metallic alloy $\text{Fe}_{40}\text{Ni}_{40}\text{P}_{14}\text{B}_6$. (●) As-received, and annealed at (□) 590, 10 min, (△) 600 K, 10 min, (○) 610 K, 10 min.

assess microstructural changes associated with the heat treatment. Thus the changes in $\Delta\rho$ might be taken here to characterize changes in the ordering and the atomic rearrangements involved during this annealing stage I. In this stage, the energy, E_{ind} , activating the induction prior to crystallization is related to the drop in the resistivity by

$$\Delta\rho_T = A \exp(-E_{\text{ind}}/KT) \quad (1)$$

where T is the absolute temperature and K is

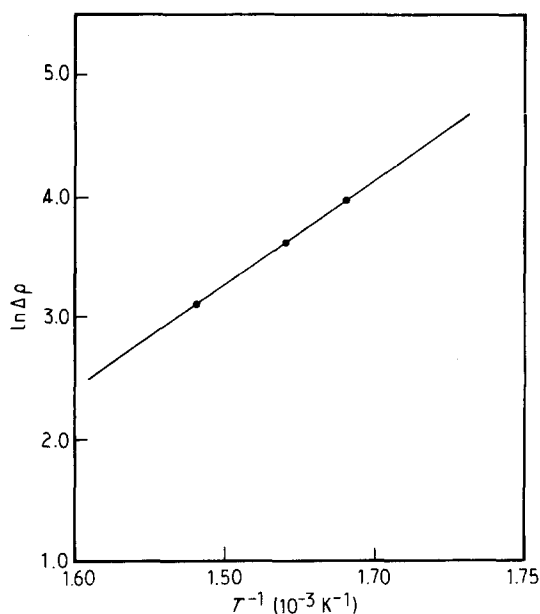


Figure 2 Determination of the activation energy characterizing the induction stage, obtained from Fig. 1 for the amorphous metallic alloy $\text{Fe}_{40}\text{Ni}_{40}\text{P}_{14}\text{B}_6$.

Boltzmann's constant. A plot of $-\ln\Delta\rho$ versus $1/TK^{-1}$ represents a straight line (see Fig. 2). From the slope of this straight line, the activation energy, E_{ind} , was found to be (1.46 ± 0.03) eV.

3.2. The crystallization stage

To study the crystallization stage, the three samples were isothermally annealed at 640, 650 and 660 K, respectively. In every case, the value of the resistivity was recorded as a function of the annealing time (t). The results are illustrated in Fig. 3. The cross-cut method [6] was applied to determine the equivalent times and temperatures, characterizing a certain degree of change by a prescribed heat pulse.

Based on the first-order chemical rate equation, describing the structural relaxation process involved, the equivalent times and temperature giving a definite degree of reaction were represented by

$$\text{constant} = t \exp(-E_{\text{cryst}}/KT) \quad (2)$$

In Fig. 4, $\ln(\text{equivalent time of annealing})$ is plotted versus the reciprocal of the corresponding annealing temperature, as a straight line. From the slope of this linear relation the energy, E_{cryst} , activating the crystallization stage was found to be (3.58 ± 0.03) eV. This value is in agreement with a previous investigation [7], using the magnetic properties of the same sample, where the activation energy was reported to be 3.65 eV.

3.3. The vacancy formation stage

In the crystalline matrix, a sharp rise in the resistivity was observed at a temperature greater than 900 K (see

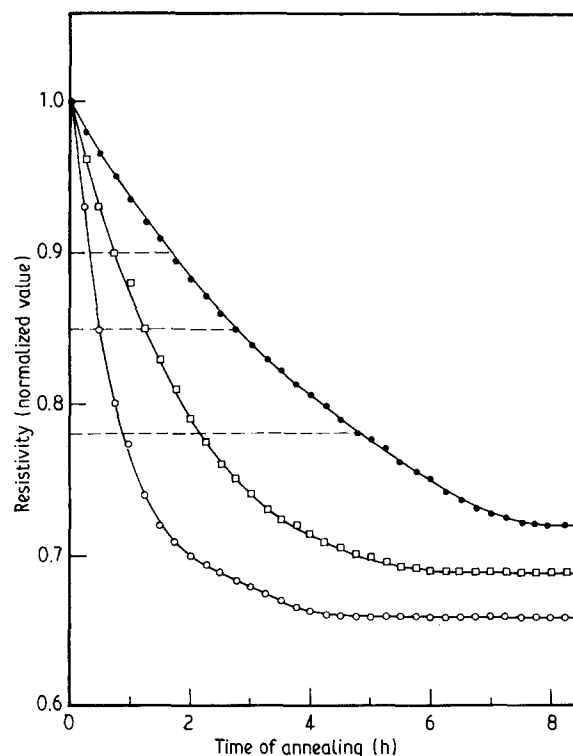


Figure 3 The normalized resistivity (at room temperature) as a function of annealing time of the amorphous metallic alloy $\text{Fe}_{40}\text{Ni}_{40}\text{P}_{14}\text{B}_6$. Annealed at (●) 640 K, (□) 650 K, (○) 660 K.

TABLE I Activation energies of the nucleation of small microcrystallites in the amorphous matrix (E_{ind}), crystallization process (E_{cryst}) and the vacancy formation in the crystallized matrix (E_{vac}) for the metglasses $\text{Fe}_{40}\text{Ni}_{40}\text{B}_{20}$, $\text{Fe}_{40}\text{Ni}_{40}\text{P}_{14}\text{B}_6$ and $\text{Fe}_{32}\text{Ni}_{36}\text{Cr}_{14}\text{P}_{12}\text{B}_6$.

Material	E_{ind} (eV)	E_{cryst} (eV)	E_{vac} (eV)	No. of atomic species
$\text{Fe}_{32}\text{Ni}_{36}\text{Cr}_{14}\text{P}_{12}\text{B}_6^{\text{a}}$	1.72	3.96	2.15	5
$\text{Fe}_{40}\text{Ni}_{40}\text{P}_{14}\text{B}_6^{\text{b}}$	1.46	3.58	1.96	4
$\text{Fe}_{40}\text{Ni}_{40}\text{B}_{20}^{\text{a}}$	0.92	3.46	1.84	3

^a Data obtained from [6].

^b Present work.

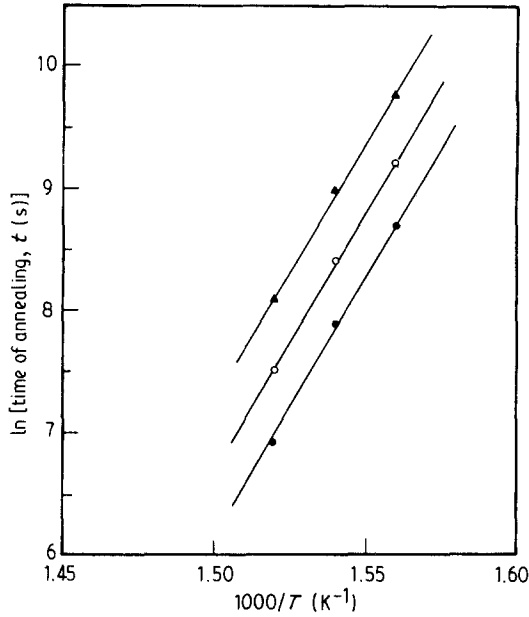


Figure 4 Equivalent times and temperatures characterizing particular states of crystallization obtained from cross-cuts in Fig. 3.

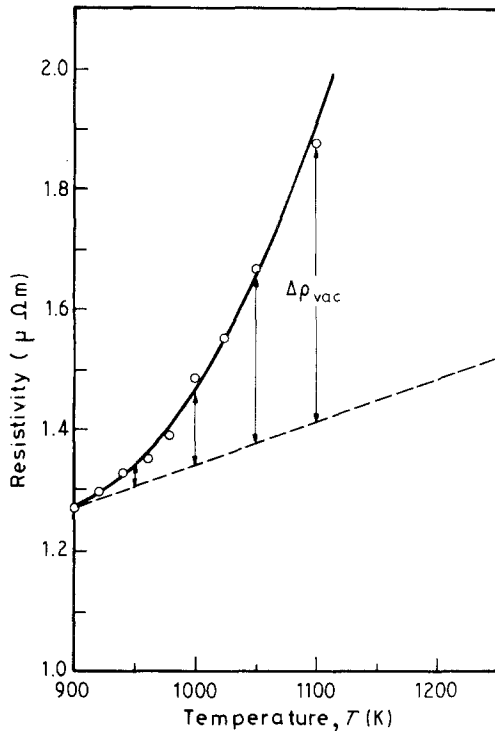


Figure 5 The change in the electrical resistivity with the temperature due to vacancy formation at higher temperature in the crystallized matrix of $\text{Fe}_{40}\text{Ni}_{40}\text{P}_{14}\text{B}_6$.

Fig. 5). This was attributed [8] to the rearrangement of the atoms in this phase. In this case, the scattering cross-section of the conduction electrons was increased by increasing the vacancy concentrations. Therefore, in the temperature range 900–1100 K it was assumed that the additional increase in the resistivity was directly proportional to the increase in the vacancy concentration (ΔC_{vac}), i.e.

$$\Delta\rho \approx \Delta C_{\text{vac}} = A \exp(-E_{\text{vac}}/KT) \quad (3)$$

where E_{vac} is the minimum energy activating the vacancy formation in the crystallized matrix.

A plot of $-\ln\Delta\rho$ versus $(1/T) \text{K}^{-1}$ represents a straight line (see Fig. 6). From the slope of this straight line the values of E_{vac} and the constant A were calculated to be $(1.96 \pm 0.03) \text{ eV}$ and $7.34 \times 10^8 \mu\Omega \text{ m}$, respectively. The latter value is one order of magnitude greater than the corresponding value obtained for the metallic glass $\text{Fe}_{32}\text{Ni}_{36}\text{Cr}_{14}\text{P}_{12}\text{B}_6$ [6].

In Table I, the values of the activation energies presented in this report were collected together with the corresponding data obtained for the amorphous and crystalline $\text{Fe}_{40}\text{Ni}_{40}\text{B}_{20}$ and $\text{Fe}_{32}\text{Ni}_{36}\text{Cr}_{14}\text{P}_{12}\text{B}_6$ metallic alloys for comparison. It is clear that the energy activating the crystallization process was increased by increasing the atomic species. This effect was found by Luborsky [9], when he studied the crystallization process of some Fe–Ni metallic alloys.

From the results, we conclude that adding phosphorus and/or chromium atoms to the compound $\text{Fe}_{40}\text{Ni}_{40}\text{B}_{20}$ would deactivate the vacancy formation. However, it is worth mentioning that the values of the first- and second-order thermal coefficients of resistiv-

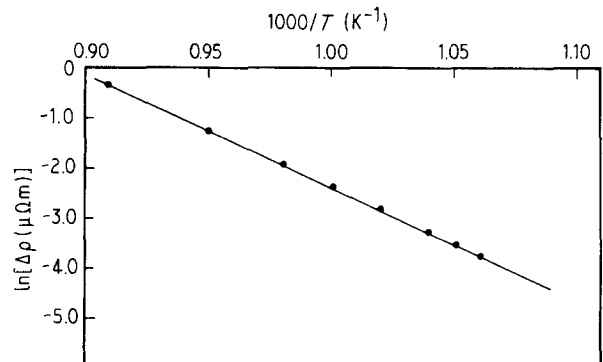


Figure 6 Determination of the minimum activation energy for the vacancy formation in the crystallized matrix of $\text{Fe}_{40}\text{Ni}_{40}\text{P}_{14}\text{B}_6$.

ity, in the crystallized matrix of the examined material (see [8]), do not obey this criterion.

References

1. J. RIVAS, M. A. LOPEZ-QUINTELA, F. WALZ and H. KRONMÜLLER, *Phys. Status Solidi (a)* **111** (1989) 611.
2. E. HUIZER and A. VAN DEN BEUKEL, *Acta Metall.* **35** (1987) 2843.
3. J. R. COST and J. T. STANLEY, *Scripta Metall.* **15** (1981) 407.
4. A. L. GREER and F. SPAEPEN, *Ann. NY Acad. Sci.* **371** (1981) 218.
5. A. VAN DEN BEUKEL, S. VAN DER ZWAAG and A. L. MULDER, *Acta Metall.* **32** (1984) 1895.
6. S. SALEH and M. A. ZAKI EWISS, *Phys. Status Solidi (a)* **117** (1990) K133.
7. S. SALEH, PhD thesis, Faculty of Science, University of Cairo (1982).
8. M. A. ZAKI EWISS and S. S. SALEH, *Phys. Status Solidi (a)* **122** (1990) K63.
9. F. E. LUBORSKY, *Mater. Sci. Engng* **28** (1977) 139.

*Received 8 June
and accepted 5 September 1990*